

DiffFaceSketch: High-Fidelity Face Image Synthesis with Sketch-Guided Latent Diffusion Model

Yichen Peng[†] Chunqi Zhao[‡] Haoran Xie[†] Tsukasa Fukusato[‡] Kazunori Miyata[†]

[†]Japan Advanced Institute of Science and Technology

[‡]The University of Tokyo

yichen.peng@jaist.ac.jp

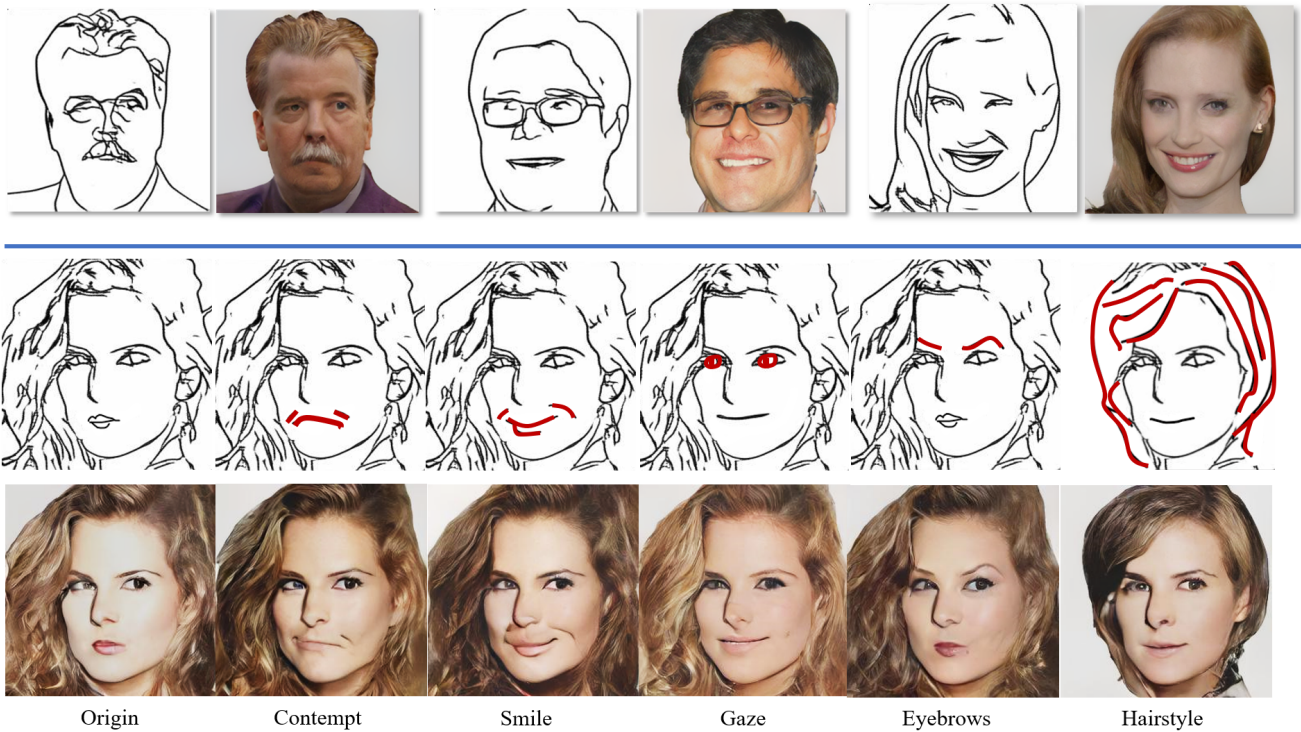


Figure 1. A Sketch-Guided Latent Diffusion Model (SGLDM) synthesizes high-quality face images with high consistency of input sketches. SGLDM enables users to simply edit face images such as different expressions, facial components, hairstyle, etc. The edited strokes are highlighted in red.

Abstract

Synthesizing face images from monochrome sketches is one of the most fundamental tasks in the field of image-to-image translation. However, it is still challenging to (1) make models learn the high-dimensional face features such as geometry and color, and (2) take into account the characteristics of input sketches. Existing methods often use sketches as indirect inputs (or as auxiliary inputs) to guide

the models, resulting in the loss of sketch features or the alteration of geometry information. In this paper, we introduce a Sketch-Guided Latent Diffusion Model (SGLDM), a LDM-based network architect trained on the paired sketch-face dataset. We apply a Multi-Auto-Encoder (AE) to encode the different input sketches from different regions of a face from pixel space to a feature map in latent space, which enables us to reduce the dimension of the sketch input while preserving the geometry-related information of

local face details. We build a sketch-face paired dataset based on the existing method that extracts the edge map from an image. We then introduce a Stochastic Region Abstraction (SRA), an approach to augment our dataset to improve the robustness of SGLDM to handle sketch input with arbitrary abstraction. The code and dataset will be released in the project page. <https://puckikk1202.github.io/difffacesketch2023/> The evaluation study shows that SGLDM can synthesize high-quality face images with different expressions, facial accessories, and hairstyles from various sketches with different abstraction levels.

1. Introduction

Synthesizing images, especially human faces, from a monochrome sketch is one of the most fundamental tasks in the image-to-image translation manner. It benefits various applications such as character design and inmate tracking. However, the sparse distributions of single-channel sketch data make feature extraction and generalization difficult. In addition, collecting paired datasets of painter’s sketches and the corresponding photographs is time-consuming and labor-intensive. It is challenging for the synthesis model to understand the monochrome sketch input with redundant semantic information (e.g., separated facial components, expressions, accessories, and hairstyles). GAN-based generative models [10, 14] are one of the feasible solutions for sketch-to-image generation based on semantic mask annotated datasets [2, 11]. Although they allow users to arrange facial semantics (i.e., regional-only conditions), many details may be lost or arbitrarily synthesized, such as wrinkles and mustaches. Instead of applying semantic masks, the other previous GAN-based models [3] trained using sketch-face paired datasets can directly generate (and edit) face images from monochrome sketches. However, they are unsuitable for handling local geometrical details such as accessories and expressions since no semantic information was directly specified in rough monochrome sketches. More recently, the diffusion model (DM) [8, 13, 22] and Contrastive Language-Image Pre-training (CLIP) [15] have achieved tremendous success on the text-to-image task. However, in the case of image-to-image, especially sketch-to-image, their system requires not only image input but also appropriate text inputs, and may not generate desired images, as shown in Figure 2. The other conditioning-guided DM-based models such as ILVR [4] and SDEdit [12] approached the image-to-image task by inputting an RGB image reference to control the synthesis. However, it is generally difficult to specify image details after noise injection and resampling of the query input. To maximize the generative models to learn from the paired sketch for more accurate information, in this work, we introduce a Sketch-Guided Latent Diffusion Model

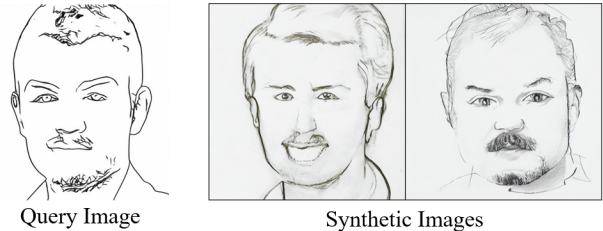


Figure 2. An example of implementing a LDM-based model, *stable diffusion* [17] with pre-trained weights. Although we inputted a single sketch (left) and texts (e.g., “a face photo” or “a portrait”), the generated results are not colored images but monochrome sketches, and do not reproduce the contours of the input sketch.

(SGLDM), an LDM-based network architect trained using a sketch-face dataset. The LDM is exceptional at flexible and high-quality inference with different conditions, we apply LDM as a backbone for our sketch-guided image synthesis training. We apply a Multi-Auto-Encoder (AE) to encode query sketches from the pixel space into feature maps in the latent space of the image feature, which enables us to reduce the dimension of the sketch input while preserving the geometrical-related information of face local details. Moreover, we apply a 2-Stage train process to achieve a better distribution mapping between the sketch and image domains. Since different people focus on different facial regions, this often leads to different levels of abstraction in the input sketch. For example, some people focus on the details of the eyes, while others focus on the mouth. To access sketch data with different levels of abstraction, we introduce a data-augmentation method, named *Stochastic Region Abstraction* (SRA) to improve the robustness of SGLDM, while sketch data is extracted from Celeba-HQ using sketch simplification methods [20, 21]. The evaluation study shows our model can generate natural-looking face images from sketches with different levels of detail. In addition, SGLDM also enables users to synthesize desired face images (in the resolution of 256×256) with different expressions, facial accessories, and hairstyles via a monochrome sketch (see Figure 1). In short, our main contributions are summarized as follows.

- We proposed SGLDM, a sketch-input-only model, which trained via a 2-Stage training process to synthesize faces with high quality and input consistency.
- We introduced SRA, a data augmentation strategy for synthesizing convincing faces from input sketches in different levels of abstraction.
- We verified the SGLDM achieves superior scores in various metrics compared to the state-of-the-art methods and is sufficiently robust enough to generate the intended face images.

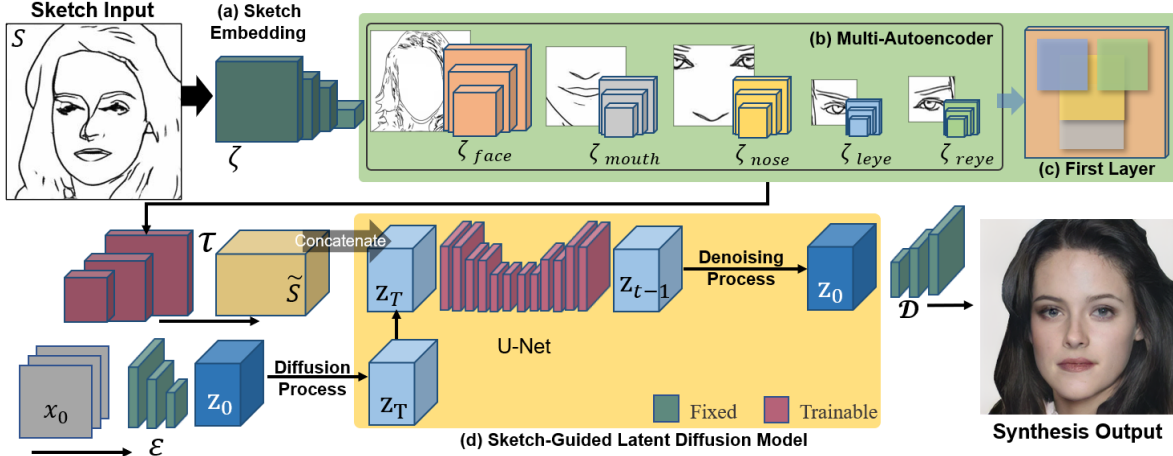


Figure 3. The framework of SGLDM. In the sketch embedding stage (a), given a sketch input S , a pretrained sketch encoder ζ encodes S into a feature vector S' . The decoder θ then decodes S' into a feature map \tilde{S} . In the latent denoising stage (b), the random latent code Z_T is concatenated by the feature map \tilde{S} and denoised to Z_0 by a U-Net. Finally, the output latent code Z_0 is decoded by a decoder \mathcal{D} to the final output.

2. Related Work

2.1. Sketch-based Image Synthesis

Image synthesis from sketches has been studied extensively over the last decade. From the beginning, sketch-to-image was treated as an image-to-image translation task, and researchers tried to train the deep learning-based network to eliminate the domain gap between monochrome sketches and RGB images. Some supervised GAN-based generative models, such as Pix2Pix [31] and Pix2pixHD [24], require paired sketch-image datasets constructed by extracting the edge map of real images to train the models. To improve the performance of mapping the image domain into the sketch domain, a large number of pairwise sketches and photos are required. Then, various dataset such as Sketchycoco [6], which categorize objects into different classes, have been released. The facial sketch image dataset is even less accessible, such as the CUHK Face Sketches [25, 30]. On the other hand, unsupervised image-to-image has been introduced in some other works (e.g., CycleGAN [31], DualGAN [28]). More recently, as the disentangled representation of StyleGAN’s $w+$ space has developed strongly, sketch-to-sketch is also treated as a style transfer task, for example, DualStyleGAN [26] and Pixel2Style2Pixel [16]. However, the end-to-end GAN-based models suffer from unstable training and are easily overfitted to a specific dataset, which limits the variety of synthesis results. Therefore, inspired by the recent outperformance of LDM in conditional image synthesis tasks, we propose SGLDM to enable high-quality face synthesis with high input consistency.

2.2. Diffusion Models

More recently, diffusion and score-based models have flourished as powerful image synthesis models, the backbone of which is a U-Net [18] that has achieved remarkable success in terms of diversity, quality, training stability, and module extensibility. Previous work [8, 22] have shown out-performance, especially in unconditional image synthesis. However, the high cost of computational resources limits the resolution of the synthesized images. Fortunately, thanks to the contribution of [17], the image is first coded from high-dimensional RGB space into a low-dimensional feature code in latent space. The latent code is then used to process the forward and backward diffusion procedures. Moreover, its good modular extensibility makes it possible to deal with image-to-image tasks such as image inpainting, semantic mask-to-image, layout-to-image, etc [17]. Other than modifying the network architect of a DM-based model, ILVR [4] and SDEdit [12] proposed the conditioning-guide sampling algorithms to tackle the image-to-image task, which required a blurry RGB reference as input to iteratively guide the sampling. However, they failed to specify image detail due to the blurred conditioning. On the other hand, for the sketch-to-image task, however, the main problem is the lack of semantic information in the monochrome sketch itself. Therefore, the sketch-to-image task via DM always requires additional input, such as a redundant text prompt. To this end, inspired by GAN-based sketch-to-image architecture [3], we apply a *Multi-Auto-Encoder* (AE) to encode the input sketch as a condition to guide the LDM denoising process. We also introduce a data augmentation method, SRA, to provide flexibility in managing sketches with different levels of abstraction.

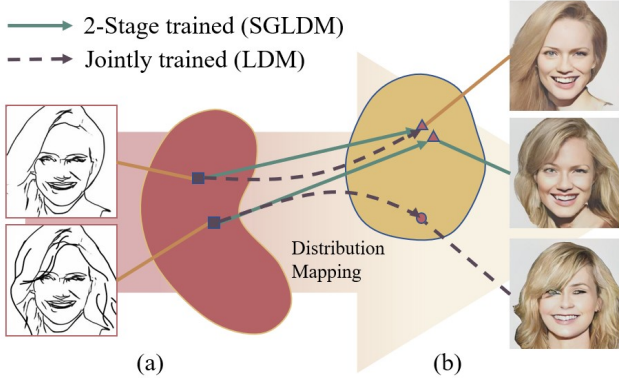


Figure 4. The different feature distribution mapping between jointly trained conditional embedding (dashed line) and the separately trained conditional embedding (solid line), from the sketch (a) to the image (b) domain.

3. Method

In this section, we first give an overview of our method in [subsection 3.1](#). We then introduce the preliminaries of DDPM and LDM in [subsection 3.2](#). The details of our framework and implementation will be discussed in [section 4](#).

3.1. Overview

Our goal is to synthesize a high-quality face image with high input consistency of the input sketch. We assume that the feature distribution of the monochrome sketches in the dataset is much more irregular and sparse than that of the RGB images. Jointly training a sketch embedding to map the sketch domain to the image domain may result in an unsmooth distribution (see [Figure 4](#)(dashed line)). Therefore, we implemented a 2-stage training method to optimize the distribution mapping between the sketch and image domains, as shown in [Figure 4](#)(solid line). More details can be found in [section 4](#).

3.2. Latent Diffusion Model

Denosing Diffusion Probabilistic Models (DDPMs or DMs) are similar to GAN and VAE, which are a new family of generative models. The key idea of DDPMs is that they randomly add noise to the initial ground true data x_0 gradually to distribute the data following a Markov chain to mimic the diffusion in non-equilibrium thermodynamics, which can be modeled as:

$$q(x_t|x_{t-1}) := \mathcal{N}(x_t; \sqrt{1 - \beta_t}x_{t-1}, \beta_t I), \quad (1)$$

where $t \sim [1, T]$ is a scheduled according to a pre-defined variance schedule $\{\beta_t \in (0, 1)\}_{t=1}^T$, They then implement and train a U-Net to learn the backward diffusion process, which can be written as:

$$q(x_t|x_0) = \mathcal{N}(x_t; \sqrt{\bar{\alpha}_t}x_0, (1 - \bar{\alpha}_t)I), \quad (2)$$

where $\bar{\alpha}_t := \prod_{i=1}^t (1 - \beta_i)$. Thus, x_t can be considered as a linear combination of the initial ground true data x_0 , and $\epsilon \sim \mathcal{N}(0, I)$. Then x_t can be simplified as:

$$x_t = \sqrt{\bar{\alpha}_t}x_0 + \sqrt{(1 - \bar{\alpha}_t)}\epsilon \quad (3)$$

The reverse process starts from x_T , which is close to an isotropic Gaussian $\mathcal{N}(0, I)$ when T is theoretically large enough. The U-Net then is trained to predict x_{t-1} from x_t by estimating the true posterior $q(x_{t-1}|x_t)$. This process can be modeled as:

$$p_\theta(x_{t-1}|x_t) = \mathcal{N}(x_{t-1}; \mu_\theta(x_t, t), \Sigma_\theta(x_t, t)). \quad (4)$$

To design the loss function, Ho et al. [8] suggested simplifying the equation by re-parameterizing the Gaussian noise term to predict ϵ_t instead since x_t is given in the training phase, where

$$\mu(x_t, t) = \frac{1}{\sqrt{\alpha_t}}(x_t - \frac{1 - \alpha_t}{\sqrt{1 - \bar{\alpha}_t}}\epsilon_\theta(x_t, t)) \quad (5)$$

After simplification, the loss L_{DM} can be written as:

$$L_{DM} = \mathbb{E}_{t \sim [1, T], x_0, \epsilon_t} [\|\epsilon_t - \epsilon_\theta(x_t, t)\|^2] \quad (6)$$

More recently, to reduce the computational cost, LDM has been proposed by Rombach et al. [17]. They have observed that the feature that contributes to the perceptual detail and conceptual semantic relevance remains in the latent code after being convoluted by the neural network of the AE model. Thus, a pre-trained encoder ε is implemented to encode the image $x \in \mathbb{R}^{H \times W \times 3}$ in high dimensional RGB space into a lower dimensional latent code $z = \varepsilon(x) \in \mathbb{R}^{h \times w \times 3}$. Then a pre-trained decoder \mathcal{D} decodes the images from the latent code $\tilde{x} = \mathcal{D}(z)$. So the loss term $Loss_{LDM}$ can be switched into:

$$L_{LDM} = \mathbb{E}_{t \sim [1, T], \varepsilon(x), \epsilon_t} [\|\epsilon_t - \epsilon_\theta(z_t, t)\|^2] \quad (7)$$

4. Sketch-guided Latent Diffusion Model

4.1. Framework

Our goal is to synthesize faces following the given sketch input. To this end, we consider sketch as a condition to guide the model while denoising. [Figure 3](#)(a, d) shows the framework of SGLDM. Inspired by Rombach et al. [17], we implement an LDM to lower the computational cost as well. And based on our sketch-conditioning pairs, the training loss L_{SGLDM} of the conditional LDM can be written as:

$$L_{SGLDM} = \mathbb{E}_{t \sim [1, T], \varepsilon(x), \epsilon_t} [\|\epsilon_t - \epsilon_\theta(z_t, t, \tau_\theta(\tilde{S}))\|^2] \quad (8)$$

where \tilde{S} is a sketch feature encoded by a pre-trained sketch encoder $\zeta(S)$ from the input sketch S . And τ_θ is a decoder to

estimate a conditional map for $\varepsilon(x)$ to reverse the diffusion process. Noted that τ_θ and ϵ_θ are trained simultaneously.

Instead of simply jointly training a sketch encoder to provide a conditional feature map for Z_T to process denoising, we construct a *Conditioning Module* by pretraining a *Multi-AE* network architecture. Inspired by works that separated global face into parts for the local networks such as DeepFaceDrawing [3], APDrawGAN [27], and MangaGAN [23], the overall encoder ζ consists of 5 partial encoders $\zeta = \{\zeta_{leye}, \zeta_{reye}, \zeta_{nose}, \zeta_{mouth}, \zeta_{face}\}$, shown as Figure 3(b, c).

4.2. 2-Stage Training Strategy

We adopt a 2-stage process for training. In sketch embedding stage, the *Conditioning Module* is pre-trained by optimizing the sum-up MSE loss $L_{Multi-AE}$ of every single partial encoder, written as:

$$L_{Multi-AE} = \left\| \sum_{\zeta_i \in \zeta} \zeta_i(x) - x \right\|_2 \quad (9)$$

There are 2 reasons for pre-training a *Multi-AE* first rather than joint training the sketch encoders to provide a conditional feature map for the SGLDM: (1) In order for the model to learn a better mapping relationship between 2 different domain data distributions of sketch and face, so as to achieve a smoother fused domain distribution space (see Figure 4). (2) To cut loads of computation cost required for training, 2-stage training separates the trainable parameters of models in each stage, thus facilitating model optimization. We train our LDM in the second stage. To further improve the robustness of SGLDM to different sketches, we adopt the *arbitrarily masking conditional training strategy* in training inspired by *Masked Autoencoder* [7], which masks random patches of the input and let the model reconstruct it automatically. In our case, since the sketch encoder ζ is pre-trained, we randomly mask out the conditioning feature map S to train the denoising U-Net.

4.3. Stochastic Region Abstraction Data Augmentation

To build our training dataset, we use high-quality 1,0000 face images from Celeba-HQ dataset [11]. We first clear up the background of the photos, as shown in Figure 5(a,b). Next, we utilize *sketch simplification* [20, 21] to generate edge maps of faces. To enhance the robustness of SGLDM to manage sketch inputs with arbitrary abstraction, we introduce SRA to a augment the dataset. We observed that the abstraction levels of the extracted edge maps depend on the image resolution. Then, we resized the original photos into 128×128 , 256×256 , and 512×512 resolutions respectively (see Figure 5(left-bottom)), and augmented our sketch dataset. The red box highlighted a clear difference in different abstraction levels in the regions of hair and eyes. More-

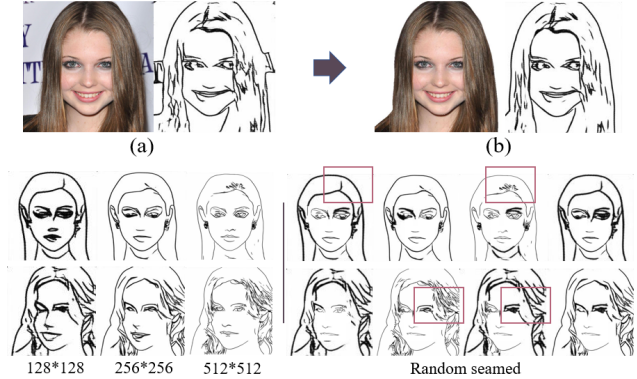


Figure 5. The original image in Celeba-HQ and its extracted edge map (a), and the result of paired data after cleaning up the background (b). Sketch simplification results from 3 different resolutions faces (left-bottom). And the random seamed data samples (right-bottom).

over, following our *Multi-AE* related region of every single encoder, we crop the edge maps into 5 different pieces and randomly combine them back together to a new edge map with random seams at different abstraction levels, showing as Figure 5(right-bottom). We finally utilized 8k images for training, 1k for validating, and 1k for testing.

5. Experiment and Results

We conduct several experiments to verify the quality and sketch input consistency of SGLDM’s synthetic face images.

5.1. Implementation

Both stages of SGLDM are trained on a single NVIDIA RTX3090 GPU. In stage one *Multi-AE* training, the training is performed for 500 epochs with an Adam optimizer with $\beta_1 = 0.9, \beta_2 = 0.999$, and batch size 64. The dimensions of the latent space of every AE are the same at 512. In stage two, our SGLDM is trained 300 epochs with an Adam optimizer as well, but the batch size is 8. The feature map of the sketch embedding has 8 channels, plus 3 channels of the LDM latent size, our denoising U-Net input is 11 channels of latent code and the output is 3 channels.¹

5.2. Quantitative Comparisons

We compare SGLDM with several state-of-the-art image-to-image translation methods on the sketch2face task (pip2pixHD [24], pix2pix [31], DeepFaceDrawing [3], pixel2style2pixel (Psp) [16], and Palette [19]). We re-trained most of the models on our 10K faces dataset picked from celeba-HQ in the same training settings. We directly implement the pre-trained weight based on 512×512 of DeepFaceDrawing.

¹Codes, Dataset, and pre-trained models are coming soon.

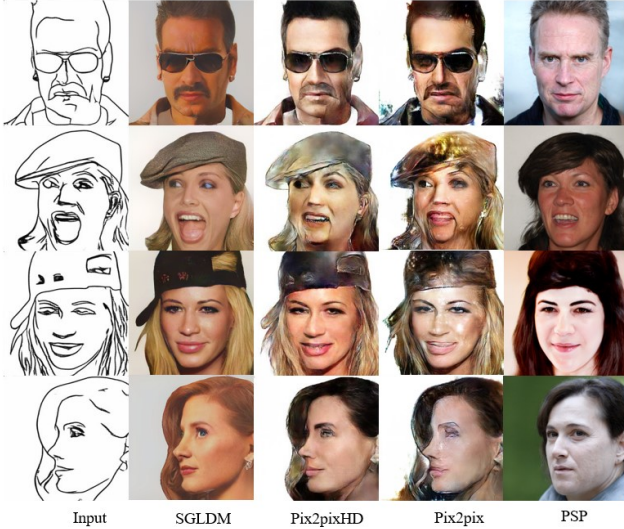


Figure 6. Examples of corner cases of sketch input which carried glasses, hat, or side face.

For the overall quality of results from different competing methods, as shown in Figure 11, SGLDM synthesizes more realistic faces while more faith in the input sketch. Pix2pix, Pix2pixHD and DeepFaceDrawing, however, trended to synthesize noisy faces when faces’ sketches are not facing straight forward, such as the third and the last columns. Note that DeepFaceDrawing additionally required a condition to control the gender of synthetic faces, so we prepare both of the results. Although Psp achieved higher quality results visually than other methods, their methods showed poor fidelity of the sketch. Besides, Palette, one DM-based image-to-image method, failed to synthesize convincing faces from sketch-only input. To our knowledge, there is no state-of-the-art DM-based pipelines that rely only on monochrome sketch input, and most of them are based on text2image, segmap2image, or image inpainting pipelines fused with sketch input (e.g., [9]).

Next, we compared SGLDM, Pix2pixHD, and Psp which have similar fidelity results (see Figure 12). The black strokes on the right are input sketches to synthesize the left face images, and the red strokes behind the black strokes are filtered versions of the synthesized images using Adobe Photoshop’s *sketch filter* [1]. From the results, we confirm that SGLDM can synthesize noiseless faces maintaining maximum consistency with the input sketch, except for some facial details such as nasolabial folds. Figure 6 shows examples of generated face images with expressions, accessories, and hairstyles. Our method achieves a better balance between the visual quality and the consistency of inputs.

We additionally conduct a user study to compare the visual quality and the input consistency of three methods: SGLDM, Pix2pixHD, and Psp. Note that Pix2pix was not

Table 1. Preference result of user study.

Method	Quality	Fidelity
Pix2pixHD [24]	17%	27%
Psp [16]	37%	2%
Ours (SGLDM)	46%	71%

included since its visual quality is similar to Pix2pixHD. Participants were asked to choose their preferences between three types of synthetic face images generated from different models for both visual quality and input consistency. From Table 1, we confirmed that face images synthesized by SGLDM achieve the highest preference for input consistency and visual quality not dissimilar to Psp.

5.3. Qualitative Evaluation

For the input consistency, we calculated the recall ratio (REC) between the black and red strokes (see Figure 12). In addition, as the visual differences in the output are minimal with different resolutions of input sketches (as mentioned in subsection 4.3), we prepared input sketches by manually erasing some strokes from the original sketches, and generated face images (see Figure 7). From these results, we confirmed that SGLDM is robust enough to handle rough sketches with different abstraction levels.

We also conducted an ablation study to compare the metrics scores between joint training & 2-Stage training methods and to verify the validity of our SRA strategy, as shown in Table 2 (lower-rows). We observed that the scores of SGLDM trained via joint training methods showed a similar performance of Pix2pixHD. Although SGLDM trained on the single abstraction level dataset (without SRA) shows the best performance on highly detailed sketch input (low abstraction), it declined significantly under higher abstraction inputs, as shown in Figure 8 (rightmost column, downward). From the results, both separate training and data augmentation methods improved the overall performance of SGLDM on various sketch inputs (see Figure 8 (second column)).

5.4. Editing Capability

We considered the usefulness of face editing. Figure 9 shows examples of partial editing (a,b) hair style of both males and females, (c) the earrings, and (d) expressions. In addition, we compared the synthetic faces of the 2-Stage trained model and the jointly trained model (see Figure 8). It illustrated that the 2-stage trained SGLDM is more robust than the jointly trained SGLDM, which turns into a different

Table 2. **Quantitative comparisons.** We applied the FID (\downarrow) score to measure the synthetic faces quality, the LPIPS (\downarrow) scores to evaluate the consistency between real faces and synthesized results, and a recall ratio (REC \uparrow) to evaluate the input consistency.

Method	Low abstraction			Mid abstraction			High abstraction		
	FID \downarrow	LPIPS \downarrow	REC \uparrow	FID \downarrow	LPIPS \downarrow	REC \uparrow	FID \downarrow	LPIPS \downarrow	REC \uparrow
Pix2pix [31]	53.67	0.20	0.54	59.46	0.23	0.50	63.45	0.28	0.51
Pix2pixHD [24]	51.23	0.18	0.62	53.71	0.22	0.55	60.23	0.25	0.53
Psp [16]	83.48	0.29	0.37	83.32	0.26	0.45	85.54	0.28	0.48
SGLDM <i>joint training</i>	46.28	0.20	0.65	48.62	0.23	0.54	50.33	0.26	0.51
SGLDM w/o SRA	38.57	0.17	0.77	48.87	0.26	0.51	57.76	0.29	0.48
Ours (SGLDM)	43.58	0.22	0.71	45.46	0.24	0.59	46.83	0.24	0.57

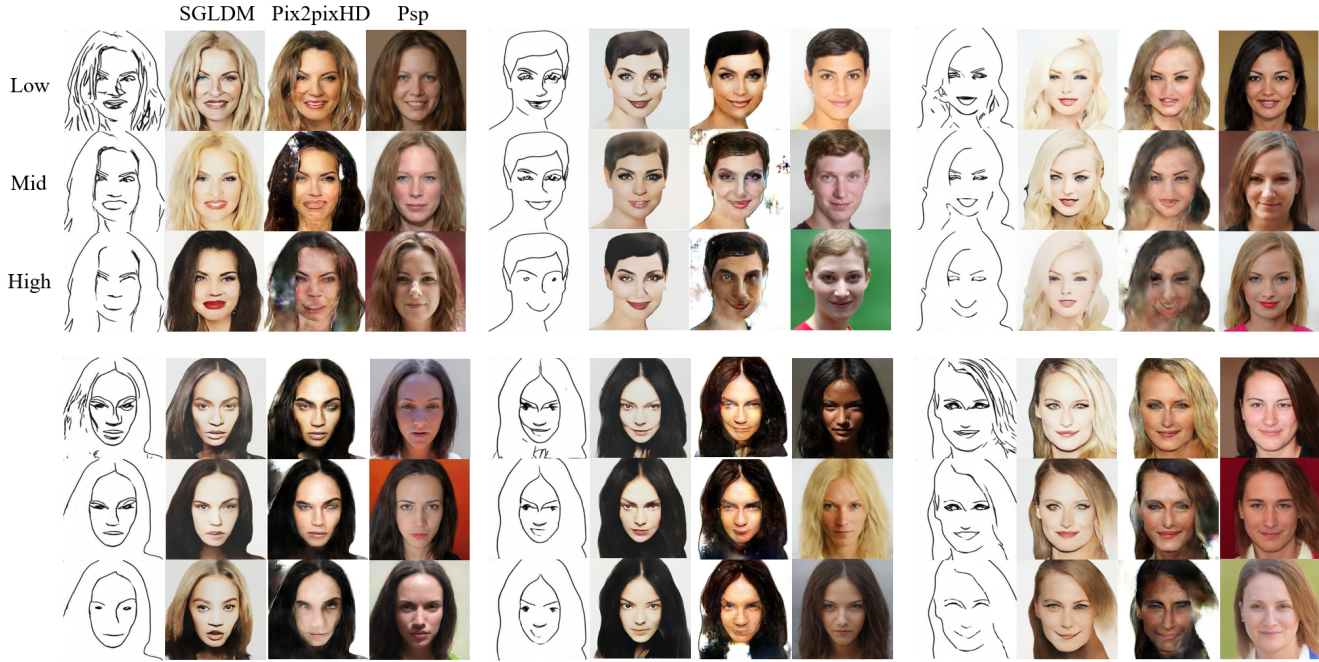


Figure 7. The comparison synthetic results in different sketch inputs with three abstraction levels.

identity easily after editing, see Figure 8 (third column, upward). As a result, SGLDM is sufficiently robust enough to edit the intended face at will on the synthetic results.

6. Limitations & Future work

Although SGLDM achieves high consistency with input sketches, the synthesized result tends to be too strongly affected by the input sketches. That is, noise and artifacts might be generated when inputting extremely poor sketches, as shown in Figure 10. To solve this issue, some trade-off methods or algorithms will be required to keep the balance between inputs' consistency and outputs' convincibility. In addition to monochrome sketch input, we plan to consider a method of inputting several color cues to handle color information such as skin and hair regions. Moreover, we evaluated SGLDM's performance on the face synthesizing

task. We believe that a similar framework can also be applied into other sketch-image tasks by changing the training dataset such as LSUN [29] and AFHQ [5]. And SRA can simply augmented each dataset to enhance the robustness of each model.

In this paper, although we implemented an LDM-based method to reduce the computation cost, SGLDM (i.e., the training and the sampling stage) is still computationally heavier than GAN-based models. In the training stage of a 256×256 model, the maximum batch size on a single NVIDIA RTX3090 is 8, while a 512×512 model's maximum batch size is only 1. In the sampling stage, the average time cost for one image is around 15.2 seconds. Although it can be cut down to around 5 to 6 seconds when using DDIM sampling strategy, the current implementation is still difficult to incorporate into a real-time interactive GUI.

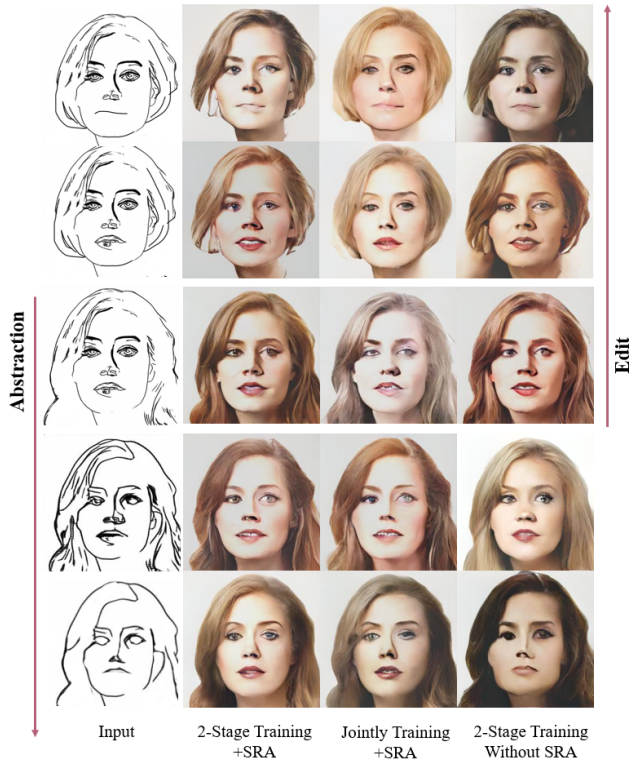


Figure 8. The synthetic faces of ablation study.

7. Conclusion

This paper has proposed SGLDM, a LDM-based architect face synthesizing model with a multi-AE to encode the query sketch as a conditional map while preserving the geometrical-related information of facial local details. We also introduced SRA, a data-augmentation strategy which enables the models to deal with sketch input with different abstraction levels. We conducted experiments to verify that SGLDM can synthesize high-quality face images with high input consistency. Moreover, SGLDM is robust enough to edit the synthetic results with different expressions, facial accessories, and hairstyles.

References

- [1] Adobe Systems Inc. Photo to pencil sketch. <https://www.adobe.com/creativecloud/photography/discover/photo-to-pencil-sketch.html>, 2022. 6
- [2] Holger Caesar, Jasper R. R. Uijlings, and Vittorio Ferrari. Coco-stuff: Thing and stuff classes in context. In *Proceedings of IEEE/CVF Conference on Computer Vision and Pattern Recognition (CVPR)*, pages 1209–1218, Salt Lake City, UT, USA, 2018. IEEE. 2
- [3] Shu-Yu Chen, Wanchao Su, Lin Gao, Shihong Xia, and Hongbo Fu. Deepfacedrawing: Deep generation of face

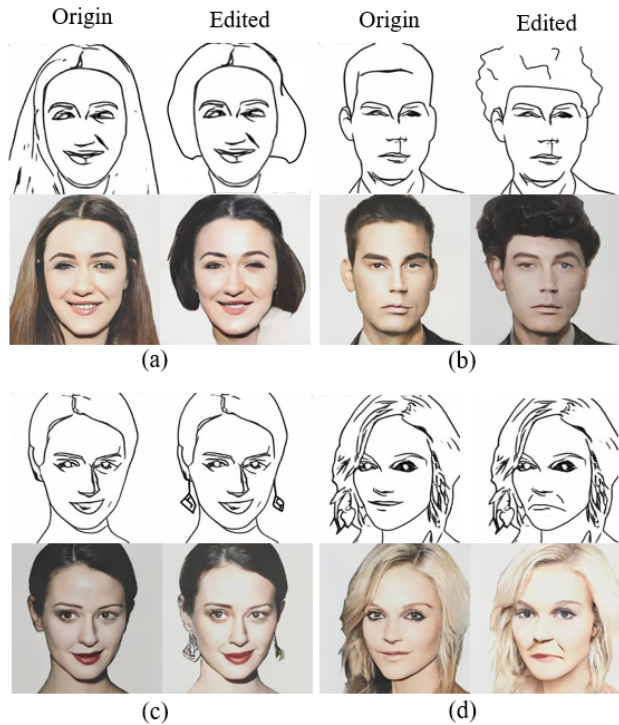


Figure 9. Examples of face editing with SGLDM. (a,b) hairstyles, (c) earrings, and (d) expression.



Figure 10. Less successful examples generated from the low-quality sketch inputs. Except for the second sketch from the right, the input sketches are from [3].

- images from sketches. *ACM Transactions on Graphics*, 39(4):72:1–72:16, 2020. 2, 3, 5, 8
- [4] Jooyoung Choi, Sungwon Kim, Yonghyun Jeong, Youngjune Gwon, and Sungroh Yoon. ILVR: conditioning method for denoising diffusion probabilistic models. *CoRR*, abs/2108.02938, 2021. 2, 3
- [5] Yunjey Choi, Youngjung Uh, Jaejun Yoo, and Jung-Woo Ha. Stargan v2: Diverse image synthesis for multiple domains. In *Proceedings of the IEEE Conference on Computer Vision and Pattern Recognition*, pages 8188–8197, Seattle, WA, USA, 2020. IEEE. 7
- [6] Chengying Gao, Qi Liu, Qi Xu, Jianzhuang Liu, Limin Wang,

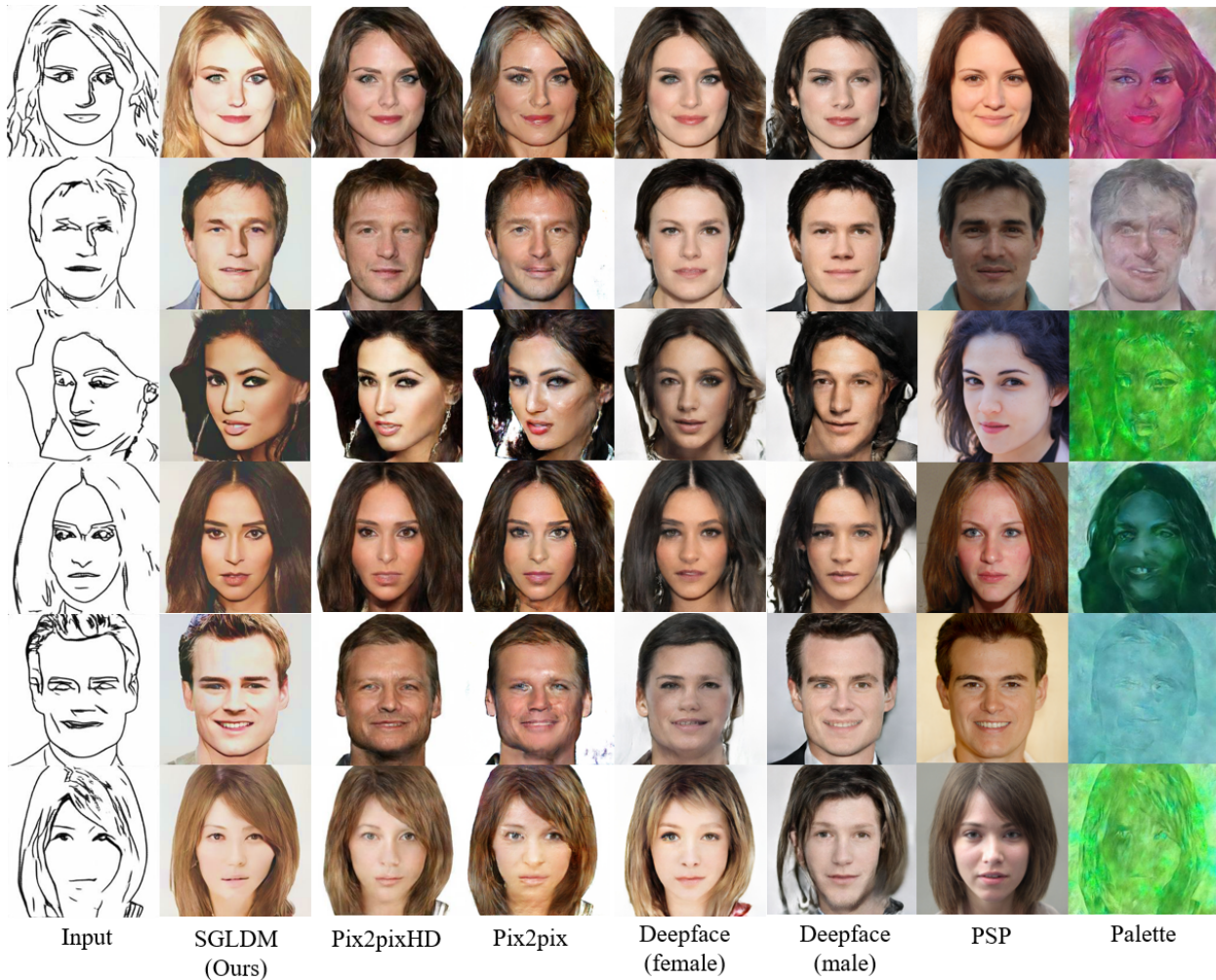


Figure 11. Qualitative comparisons of the proposed SGLDM with the state-of-the-art methods.



Figure 12. Fidelity comparisons of the proposed SGLDM with competing methods.

and Changqing Zou. Sketchycoco: Image generation from freehand scene sketches. In *Proceedings of IEEE/CVF Conference on Computer Vision and Pattern Recognition (CVPR)*, pages 5174–5183, Seattle, WA, USA, 2020. IEEE. 3

[7] Kaiming He, Xinlei Chen, Saining Xie, Yanghao Li, Piotr Dollár, and Ross B. Girshick. Masked autoencoders are scalable vision learners. In *Proceedings of IEEE/CVF Conference on Computer Vision and Pattern Recognition (CVPR)*, pages

- 16000–16009, New Orleans, LA, USA, 2022. IEEE. 5
- [8] Jonathan Ho, Ajay Jain, and Pieter Abbeel. Denoising diffusion probabilistic models. *Proceedings of Advances in Neural Information Processing Systems*, 33:6840–6851, 2020. 2, 3, 4
- [9] Daichi Horita, Jiaolong Yang, Dong Chen, Yuki Koyama, and Kiyoharu Aizawa. A structure-guided diffusion model for large-hole diverse image completion. *CoRR*, arXiv:2211.10437:1–17, 2022. 6
- [10] C. Lee, Z. Liu, L. Wu, and P. Luo. Maskgan: Towards diverse and interactive facial image manipulation. In *Proceedings of IEEE/CVF Conference on Computer Vision and Pattern Recognition (CVPR)*, pages 5548–5557, Los Alamitos, CA, USA, Jun 2020. IEEE Computer Society. 2
- [11] Cheng-Han Lee, Ziwei Liu, Lingyun Wu, and Ping Luo. Maskgan: Towards diverse and interactive facial image manipulation. In *Proceedings of IEEE/CVF Conference on Computer Vision and Pattern Recognition (CVPR)*, pages 5548–5557, Seattle, WA, USA, 2020. IEEE. 2, 5
- [12] Chenlin Meng, Yang Song, Jiaming Song, Jiajun Wu, Jun-Yan Zhu, and Stefano Ermon. Sdedit: Image synthesis and editing with stochastic differential equations. *CoRR*, abs/2108.01073, 2021. 2, 3
- [13] Alex Nichol and Pratul Dhariwal. Improved denoising diffusion probabilistic models. *Proceedings of the 38th International Conference on Machine Learning*, 139:8162–8171, 2021. 2
- [14] Taesung Park, Ming-Yu Liu, Ting-Chun Wang, and Jun-Yan Zhu. Semantic image synthesis with spatially-adaptive normalization. In *Proceedings of 2019 IEEE/CVF Conference on Computer Vision and Pattern Recognition (CVPR)*, pages 2337–2346, Long Beach, CA, USA, 2019. IEEE. 2
- [15] Alec Radford, Jong Wook Kim, Chris Hallacy, Aditya Ramesh, Gabriel Goh, Sandhini Agarwal, Girish Sastry, Amanda Askell, Pamela Mishkin, Jack Clark, Gretchen Krueger, and Ilya Sutskever. Learning transferable visual models from natural language supervision. *Proceedings of the 38th International Conference on Machine Learning*, 139:8748–8763, 2021. 2
- [16] Elad Richardson, Yuval Alaluf, Or Patashnik, Yotam Nitzan, Yaniv Azar, Stav Shapiro, and Daniel Cohen-Or. Encoding in style: a stylegan encoder for image-to-image translation. In *Proceedings of IEEE/CVF Conference on Computer Vision and Pattern Recognition (CVPR)*, pages 2287–2296, Nashville, TN, USA, 2020. IEEE. 3, 5, 6, 7
- [17] Robin Rombach, Andreas Blattmann, Dominik Lorenz, Patrick Esser, and Björn Ommer. High-resolution image synthesis with latent diffusion models. In *Proceedings of IEEE/CVF Conference on Computer Vision and Pattern Recognition (CVPR)*, pages 10684–10695, New Orleans, LA, USA, 2021. IEEE. 2, 3, 4
- [18] Olaf Ronneberger, Philipp Fischer, and Thomas Brox. U-net: Convolutional networks for biomedical image segmentation. In *Proceedings of Medical Image Computing and Computer-Assisted Intervention (MICCAI)*, pages 234–241, Cham, 2015. Springer. 3
- [19] Chitwan Saharia, William Chan, Huiwen Chang, Chris A. Lee, Jonathan Ho, Tim Salimans, David J. Fleet, and Mohammad Norouzi. Palette: Image-to-image diffusion models. In *ACM SIGGRAPH 2022 Conference Proceedings*, pages 15:1–15:10, New York, NY, USA, 2021. ACM. 5
- [20] Edgar Simo-Serra, Satoshi Iizuka, and Hiroshi Ishikawa. Mastering sketching: Adversarial augmentation for structured prediction. *ACM Transactions on Graphics*, 37(1):11:1–11:13, 2018. 2, 5
- [21] Edgar Simo-Serra, Satoshi Iizuka, Kazuma Sasaki, and Hiroshi Ishikawa. Learning to simplify: Fully convolutional networks for rough sketch cleanup. *ACM Transactions on Graphics*, 35(4):121:1–121:11, 2016. 2, 5
- [22] Jiaming Song, Chenlin Meng, and Stefano Ermon. Denoising diffusion implicit models. In *9th International Conference on Learning Representations (ICLR)*, pages 1–20, Virtual Event, Austria, 2021. OpenReview.net. 2, 3
- [23] Hao Su, Jianwei Niu, Xuefeng Liu, Qingfeng Li, Jiahe Cui, and Ji Wan. Mangagan: Unpaired photo-to-manga translation based on the methodology of manga drawing. *Proceedings of the AAAI Conference on Artificial Intelligence*, 35(3):2611–2619, 2021. 5
- [24] Ting-Chun Wang, Ming-Yu Liu, Jun-Yan Zhu, Andrew Tao, Jan Kautz, and Bryan Catanzaro. High-resolution image synthesis and semantic manipulation with conditional gans. In *Proceedings of the IEEE Conference on Computer Vision and Pattern Recognition*, pages 8798–8807, Salt Lake City, UT, USA, 2018. IEEE. 3, 5, 6, 7
- [25] Xiaogang Wang and Xiaoou Tang. Face photo-sketch synthesis and recognition. *IEEE Transactions on Pattern Analysis and Machine Intelligence*, 31(11):1955–1967, 2009. 3
- [26] Shuai Yang, Liming Jiang, Ziwei Liu, and Chen Change Loy. Pastiche master: Exemplar-based high-resolution portrait style transfer. In *Proceedings of IEEE/CVF Conference on Computer Vision and Pattern Recognition (CVPR)*, pages 7693–7702, New Orleans, LA, USA, 2022. IEEE. 3
- [27] Ran Yi, Yong-Jin Liu, Yu-Kun Lai, and Paul L. Rosin. Apdrawinggan: Generating artistic portrait drawings from face photos with hierarchical gans. In *Proceedings of IEEE Conference on Computer Vision and Pattern Recognition (CVPR)*, pages 10743–10752, Long Beach, CA, USA, 2019. IEEE. 5
- [28] Zili Yi, Hao Zhang, Ping Tan, and Minglun Gong. Dualgan: Unsupervised dual learning for image-to-image translation. In *Proceedings of IEEE International Conference on Computer Vision (ICCV)*, pages 2849–2857, Venice, Italy, 2017. IEEE. 3
- [29] Fisher Yu, Yinda Zhang, Shuran Song, Ari Seff, and Jianxiong Xiao. LSUN: construction of a large-scale image dataset using deep learning with humans in the loop. *CoRR*, abs/1506.03365:1–9, 2015. 7
- [30] Wei Zhang, Xiaogang Wang, and Xiaoou Tang. Coupled information-theoretic encoding for face photo-sketch recognition. In *Proceedings of IEEE Conference on Computer Vision and Pattern Recognition (CVPR)*, pages 513–520, Colorado Springs, CO, USA, 2011. IEEE. 3
- [31] Jun-Yan Zhu, Taesung Park, Phillip Isola, and Alexei A. Efros. Unpaired image-to-image translation using cycle-consistent adversarial networks. In *Proceedings of IEEE International Conference on Computer Vision (ICCV)*, pages 2223–2232, Venice, Italy, 2017. IEEE. 3, 5, 7